Eur. Phys. J. D (2016) 70: 207
DOI: 10.1140/epjd/e2016-70259-5

THE EUROPEAN PHYSICAL JOURNAL D

Regular Article

Benchmark for two-photon ionization of atoms with generalized Sturmian functions

Antonio I. Gómez[1,2,a], Gustavo Gasaneo[1,2], Darío M. Mitnik[2,3], Marcelo J. Ambrosio[2,3], and Lorenzo U. Ancarani[4]

[1] Departamento de Física, Universidad Nacional del Sur, 8000 Bahía Blanca, Buenos Aires, Argentina
[2] Consejo Nacional de Investigaciones Científicas y Técnicas (CONICET), Buenos Aires, Argentina
[3] Instituto de Astronomía y Física del Espacio (IAFE) and Departamento de Física, Universidad de Buenos Aires, C1428EGA Buenos Aires, Argentina
[4] Théorie, Modélisation, Simulation, SRSMC, UMR CNRS 7565, Université de Lorraine, 57078 Metz, France

Received 12 April 2016 / Received in final form 22 June 2016
Published online 18 October 2016 –

Abstract. The description with traditional methods of the single or multiple ionization of atoms and molecules by two or more successive photons requires some special treatment. Difficulties occur when a spatially non-decaying driven term appears in the Schrödinger-like non-homogeneous equation for the scattering wave function. We propose using the intrinsic physical and mathematical properties of generalized Sturmian functions to efficiently deal with the Dalgarno-Lewis second order equation. In contrast to other approaches, our methodology provides a practical way to extract the transition amplitude from the asymptotic behavior of the scattering wave function, and this without requiring any further projection onto some final approximate state. As an illustration, the hydrogen case is studied in details, for both pulsed and monochrome laser radiation fields. The successful comparison with analytical and time-dependent solutions provides a benchmark, and allows us to master the numerical aspects of the methodology. Appropriately chosen generalized Sturmian functions manage to easily reproduce the beat-type asymptotic behavior observed in the photoelectron wave function after absorption by the atom of two successive photons.

1 Introduction

In the last few years, the development of high order harmonics generation source and free electron lasers that provide ultra-intense and ultra-short VUV-XUV pulses have allowed the study of the dynamics in atomic and molecular systems on its intrinsic timescale [1–13]. The observation and control of such dynamics is a promising approach to understand and manipulate the studied system at a fundamental level. The detailed understanding of the quantum dynamics between correlated electrons is essential to determine the macroscopic properties in any natural system (as chemical reactions and solid state effects, including superconductivity) since it relates to atomic and molecular non-equilibrium processes. Such correlation effects can be most clearly investigated in processes involving single atoms. In particular, the emission of two electrons from an atom (induced by the impact of photons, by a charged particle or by a short laser pulse) has become the standard process for studies of dynamical electron correlations [14]. Recent experiments on helium with a single active electron [11,15,16], and, more recently, with two active electrons [17], motivate the development of theoretical and numerical methods that provide solutions to the related time-dependent Schrödinger equation (TDSE). Theoretical solutions with benchmark accuracy for simple systems have become critical to the understanding and prediction of experimental results that are necessarily carried out under conditions where a number of ionization channels compete with the one that is the focus of measurement. In addition, the unambiguous analysis of the wave function of the fundamental processes involved at these energies is essential for the design of future experiments. A recent example of this is the determination of the absolute intensity of a laser to unprecedented accuracy (at the 1% level), achieved using accurate theoretical data together with experimental ones for hydrogen atom [18].

As evidenced by the huge literature on the topic, obtaining an accurate theoretical description of the double ionization of the helium atom presents a measurable challenge for numerical methods. The difficulty of correctly taking into account the electron correlation in three-body scattering problems translates into discrepancies observed between several ab initio methods when looking at different processes and in different energy regimes. One of the technical obstacles encountered is the issue of how to extract quantitative scattering information from the propagated wave packet, and thus how to calculate the double ionization amplitudes and cross sections. The imposition of exact asymptotic conditions when solving the TDSE

[a] e-mail: aigmz.1985@gmail.com

on a finite domain, remains indeed a formidable task. Another very important issue is the choice of the domain size, and its discretization; a finite domain must include the internal region where the solution is of interest. This is a serious problem, for example, when dealing with two-photons double photoionization of helium [19]. Indeed, for photons with energies greater than the first ionization threshold, the second order Dalgarno-Lewis equation has a driven term (or source) that is not bound spatially since it contains the wave function associated with the single ionization. As a consequence, the scattering amplitude to be extracted from the second-order solution does not converge with increasing domain size. Our group has implemented a generalized Sturmian function methodology (GSF) [20,21] to calculate cross sections for several three-body scattering processes. One important advantage offered by the method is that the scattering amplitude is extracted directly from the wave function in the asymptotic region; this differs from other approaches which need to project the solution onto some final approximate state. Solving the first order term of the Dalgarno-Lewis perturbation series, the double photoionization of helium by one-photon absorption was investigated in reference [22] where the GSF method was shown to be numerically very efficient.

We aim to apply our GSF methodology to other and more difficult problems, such as, e.g., the double ionization of helium by two-photon absorption. As a first step, in this paper, we will focus on how one should (slightly) modify the methodology for situations where the source is not spatially limited. For this purpose, we use a one-electron test case that presents the main characteristics we want to emphasize; it allows us to understand how the methodology works and to delve into some of the numerical aspects of the general method we propose to address, i.e., the multiphoton double ionization problem in two-electron atoms. In this contribution, we study an hydrogen atom in its ground state interacting with an electric field. For above-threshold ionization (ATI), the one-photon absorption can be solved rather easily with various methods. However, the resolution of the next order involves a driven equation with a spatially unbound source (the latter involves the scattering wave function with outgoing wave condition corresponding to the ionization due to the absorption of the first photon). This fact presents a difficulty from the standpoint of the numerical implementation [19], and is the cornerstone of this contribution.

Two cases of interest are considered. First, we study the interaction with a XUV pulse in order to validate and check the pertinence of the proposed GSF scheme. This benchmark case enables us to see the most important aspects of how the methodology works, as well as highlighting the behavior of the driven term (not so obvious at first glance). It also serves as a bridge to address the second case, involving an interaction with a monochrome laser, which presents a spatially unlimited driven term in the non-homogeneous Schrödinger equation.

In this work we show that the intrinsic mathematical properties of GSFs are ideal to tackle multi-photon differential equations, in which the source does not vanish at large distances. More precisely, we use two characteristics of the generalized Sturmian basis functions. The first one is that they can be constructed with the desired asymptotic behavior, congruent with the physical problem. The second feature is that all basis functions possess the same asymptotic behavior. These properties allow one to evaluate the scattering amplitude directly from the wave function in the asymptotic region, not as a matrix element and without the need for any ad hoc assumptions as in other approaches found in the literature. We also show that, if one has previously obtained the wave function by any numerical method, those same GSF properties can be used to extract the ionization amplitude.

The rest of this paper is organized as follows. In Section 2, we present the perturbation approach to the time independent Schrödinger equation (TISE), the GSF resolution method, and the way the ionization amplitude is extracted. Section 3 provides the results for hydrogen obtained for the two cases considered (pulse and monochrome laser). A summary of the investigation is provided in Section 4.

Atomic units ($\hbar = e = m_e = 1$) are used throughout.

2 Theory and resolution method

Our theoretical approach begins with the time-dependent Schrödinger equation, and with the procedure we propose for calculating the cross section. For a general atom, we first characterize the time evolution of the system by using the Fourier representation for both wave function and the electromagnetic field (see, e.g., [23,24]). Second, we use a perturbation approach that allows us to include the absorption of photons one by one. Then, specifying the study to a one active electron case, we make a partial waves expansion to separate the angular from the radial part, and solve the coupled radial equations using the GSF method. Finally, we extract the transition amplitude directly from the asymptotic behavior of the calculated scattering wave function.

The GSF recipe is applied here to the hydrogen atom, obviously the best choice for testing different approaches, approximations and explore some of numerical aspects of the proposed general method which we plan, at a later stage, to apply for more complicated processes or atoms.

2.1 Perturbation approach to the time-independent Schrödinger equation

In order to describe the photoionization process, we use the perturbation theory, the atom interacting with a classical external electric field. For such processes, the Hamiltonian can be written as:

$$H(t) = H_0 + \lambda W(t), \tag{1}$$

where H_0 is the field-free Hamiltonian of the system, and $\lambda W(t)$ is a time-dependent perturbation which describes

the field-system coupling (λ is a small parameter). In the dipolar approximation, the interaction potential in the velocity gauge is given by:

$$W(t) = \mathbf{A}(t)\mathbf{P} = -iA(t)\hat{z}\cdot\nabla, \tag{2}$$

where $\mathbf{P}$ is the total momentum of the active particles (∇ stands hereafter for the sum $\sum_j \nabla_j$ over all electrons) and $\mathbf{A}(t)$ is the vector potential hereafter take as polarized in the $\hat{z}$ direction; $\mathbf{A}(t) = -\int \mathcal{E}(t)\, dt$, where $\mathcal{E}(t)$ is the electric field. Let $\mathcal{R}$ represent collectively all electron positions $\{\mathbf{r_j}\}$. The general solution of the TDSE is proposed to be

$$\Psi(t,\mathcal{R}) = e^{-i\omega_i t}\left[\Phi_i(\mathcal{R}) + \Phi_{\text{scatt}}(t,\mathcal{R})\right], \tag{3}$$

where $\Phi_i(\mathcal{R})$ is the wave function of the initial state of the atom with energy ω_i, $\Phi_{\text{scatt}}(t,\mathcal{R})$ is the wave function of the photoelectron. Replacing the proposal (3) into the TDSE, we obtain the driven time-dependent equation

$$\left[i\frac{\partial}{\partial t} - \omega_i - H_0 - \lambda\mathcal{F}(t)\,\hat{z}\nabla\right] \times \Phi_{\text{scatt}}(t,\mathcal{R}) = \mathcal{F}(t)\,\hat{z}\nabla\Phi_i(\mathcal{R}), \tag{4}$$

where $\mathcal{F}(t) = -iA(t)$. Now, applying a Fourier transform we obtain the driven time-independent equation

$$[\omega_{sc} - H_0]\,\overline{\Phi}_{\text{scatt}}(\omega,\mathcal{R}) - \frac{\lambda}{\sqrt{2\pi}}\int_{-\infty}^{\infty} d\omega'\,\overline{\mathcal{F}}(\omega')\,\hat{z}\nabla\overline{\Phi}_{\text{scatt}}(\omega-\omega',\mathcal{R}) = \overline{\mathcal{F}}(\omega)\,\hat{z}\cdot\nabla\Phi_i(\mathcal{R}), \tag{5}$$

where ω is the energy delivered by the field, $\overline{\mathcal{F}}(\omega)$ is the Fourier transform of $\mathcal{F}(t)$, and $\omega_{sc} = \omega + \omega_i = k_{sc}^2/2$ where k_{sc} is the wave vector of the photoelectron. Equation (5) contains the interaction with the field to all orders and, thus, all possible processes are included in $\overline{\Phi}_{\text{scatt}}(\omega,\mathcal{R})$. Introducing a perturbative expansion on the scattering wave function [25], successive orders satisfy the following system of differential equations

$$(\omega_{sc} - H_0)\,\overline{\Phi}^{(1)}(\omega,\mathcal{R}) = \overline{\mathcal{F}}(\omega)\,\hat{z}\nabla\overline{\Phi}^{(0)}(\mathcal{R}), \tag{6a}$$

$$(\omega_{sc} - H_0)\,\overline{\Phi}^{(2)}(\omega,\mathcal{R}) = \frac{1}{\sqrt{2\pi}}\int_{-\infty}^{\infty} d\omega'\,\overline{\mathcal{F}}(\omega')\,\hat{z} \times \nabla\overline{\Phi}^{(1)}(\omega-\omega',\mathcal{R}), \tag{6b}$$

$$\vdots$$

$$(\omega_{sc} - H_0)\,\overline{\Phi}^{(N)}(\omega,\mathcal{R}) = \frac{1}{\sqrt{2\pi}}\int_{-\infty}^{\infty} d\omega'\,\overline{\mathcal{F}}(\omega')\,\hat{z} \times \nabla\overline{\Phi}^{(N-1)}(\omega-\omega',\mathcal{R}), \tag{6c}$$

where $\overline{\Phi}^{(n)}(\omega,\mathcal{R})$ is the (transformed) scattering wave function at nth-order, and $\overline{\Phi}^{(0)}(\mathcal{R}) = \overline{\Phi}_i(\mathcal{R})$ is the wave function of the initial state. This is the system of driven equations that we employ to investigate multiphoton ionization processes in the ATI region. Equation (6a) corresponds to absorption of one photon: since the driven term involves a derivative of the initial ground state, it is spatially bound and the non-homogeneous differential equation can be solved by different methods; its solution should describe an outgoing photoelectron. The second order driven equation, corresponding to absorption of a second photon, includes in its driven term the solution $\overline{\Phi}^{(1)}(\omega,\mathcal{R})$ (which is not spatially bound) [26,27] through a convolution with the electric field. As the behavior of the driven term is not at all obvious, the second order equation should be given special attention; numerical schemes that can solve the first order equation are generally not directly applicable to the second order one (at least, not without including some *ad hoc* adjustment (see, e.g., Ref. [19]).

We consider hereafter the hydrogen atom (electron of coordinates $\mathbf{r}$), so that the potential in H_0 is simply $-Z/r$ with $Z = 1$. With a central potential we expand the scattering wave function in partial waves

$$\overline{\Phi}^{(n)}(\omega,\mathbf{r}) = \frac{1}{r}\sum_{lm} Y_l^m(\theta,\varphi)\;\varphi_l^{(n)}(\omega,r) \tag{7}$$

and through a standard angular projection, we obtain the system of radial driven equations

$$\left[\omega_{sc} + \frac{1}{2}\frac{\partial^2}{\partial r^2} - \frac{l(l+1)}{2r^2} + \frac{Z}{r}\right]\varphi_l^{(n)}(\omega,r) = f_{RHS}^{(n-1)}(\omega,r), \tag{8}$$

where $f_{RHS}^{(n-1)}(\omega,r)$ stands for the radial driven term corresponding to nth-order equation.

2.2 Generalized Sturmian functions method

As the GSF method has been described in details elsewhere [20,21], here we recall only the essential. For a given angular momentum l, the GSF are the solutions to the two body Schrödinger equation

$$\left[-\frac{1}{2}\frac{\partial^2}{\partial r^2} + \frac{l(l+1)}{2r^2} + \mathcal{U}(r) - E_s\right] \times S_{j,l}(E_s,r) = -\beta_{j,l}\mathcal{V}(r)\,S_{j,l}(E_s,r), \tag{9}$$

where $\beta_{j,l}$ are the eigenvalue, E_s is a parameter of the equation, $\mathcal{U}(r)$ is the auxiliary potential and $\mathcal{V}(r)$ is the generating potential. In general, the generating potential is chosen as a short range potential and determines the range and the dynamics of an inner region, while the auxiliary potential is chosen as a long-range potential which fixes the asymptotic behavior of all the solutions $S_{j,l}(E_s,r)$; for scattering studies one may choose, for example, outgoing behavior (examples of GSF, with two different energies, are shown in the top and middle panels of Fig. 10). Additionally, GSFs conform a complete basis set, orthogonal with respect to the generating potential.

To solve equation (8), we use a Sturmian representation of the solution

$$\varphi_l^{(n)}(\omega,r) = \sum_j a_{j,l}^{(n)}(\omega) S_{j,l}^{(n)}(E_s,r). \tag{10}$$

Using equation (9) with $\mathcal{U}(r) = -Z/r$ and projecting with $S^{(n)}_{i,l}(E_s, r)$ (note that for GSF complex conjugation does not apply [20]), we obtain

$$\sum_j \left[(\omega_{sc} - E_s)\,\mathcal{O}_{i,j} + \beta_j \delta_{i,j}\right] a^{(n)}_{j,l}(\omega) = b^{(n)}_i \tag{11}$$

where $b^{(n)}_i$ are given by:

$$b^{(n)}_i = \int_0^\infty dr\; S^{(n)}_{i,l}(E_s, r)\; f^{(n-1)}_{RHS}(r) \tag{12}$$

and $\mathcal{O}_{i,j}$ are the elements of the overlap matrix

$$\mathcal{O}_{i,j} = \int_0^\infty dr\; S^{(n)}_{i,l}(E_s, r)\; S^{(n)}_{j,l}(E_s, r). \tag{13}$$

Solving the matrix problem with standard numerical methods provides the coefficients $a^{(n)}_{j,l}(\omega)$.

2.3 Extraction of the ionization amplitude

When the driven terms $f^{(n-1)}_{RHS}(\omega, r)$ vanish at large distances, equation (8) can be formally solved. Denoting $H^{(n)+}_{l,\infty}(r)$ the function representing the asymptotic behavior, at large distances we have $\varphi^{(n)}_l(\omega, r) \to \mathcal{A}^{(n)}_l(\omega)\; H^{(n)+}_{l,\infty}(r)$ where $\mathcal{A}^{(n)}_l(\omega)$ is the transition amplitude. For example, for the first order one-photon ionization equation (6a), the function $H^{(n)+}_{l,\infty}(r)$ is the Coulomb function $H^+_l(r)$ with outgoing behavior [25] function

$$H^{(1)+}_{l,\infty}(r) = H^+_l(r) \propto e^{i[k_{sc}r + (Z/k_{sc})\ln(2k_{sc}r)]}. \tag{14}$$

All the GSF we use for these particular scattering processes are constructed possessing exactly the asymptotic behavior (14), so that expansion (10) reads

$$\varphi^{(n)}_l(\omega, r) \to \left(\sum_j a^{(n)}_{j,l}(\omega)\right) H^+_l(r)\,. \tag{15}$$

The ionization amplitude, for a given partial wave l, is extracted directly from the scattering wave function as a simple sum of coefficients

$$\mathcal{A}^{(n)}_l(\omega) = \sum_j a^{(n)}_{j,l}(\omega). \tag{16}$$

In relation to these amplitudes, two quantities describe the process: the differential ionization probability (DIP) that includes the pulse effects and the photoionization cross section (CS). They are given respectively by [28–31]:

$$\frac{dP_n(\omega)}{d\Omega} = \frac{4}{3}(2\pi) k_{sc} \left|C^{(n)}(\mathbf{k})\right|^2 \tag{17}$$

and

$$\frac{d\sigma_n(\omega)}{d\Omega} = \frac{2\,\pi\,\omega\,(2\,\pi\,\alpha\,I)^n\,k_{sc}}{I\,(n\,\omega)^{2n}}\,|T_n|^2\,, \tag{18}$$

where α is the fine-structure constant, I is the intensity of the electric field; the multiphoton ionization amplitude $C^{(n)}(\mathbf{k})$ includes the pulse effect, and is proportional to T_n, the compound matrix elements [31],

$$T_n = \Big\langle \overline{\Phi}^{(n)} \,|(\hat{z}\nabla)\; G_{n-1}(\hat{z}\nabla)\; G_{n-2}(\hat{z}\nabla) \ldots G_1(\hat{z}\nabla)|\, \overline{\Phi}^{(0)} \Big\rangle \tag{19}$$

where $G_n = [\omega_i + n\,\omega - H_0]^{-1}$ is the Green function.

Within our GSF framework, the explicit way of calculating the DIP and the CS is given below, separately for the one-photon ($n = 1$) and two-photon ($n = 2$) cases.

When the driven term $f^{(n-1)}_{RHS}(\omega, r)$ of equation (8) does not vanish at large distances, a special treatment is required. The process of two-photon absorption with a persistent monochromatic radiation is a physical example of this mathematical situation. Indeed, while for the first order equation ($n = 1$) the initial bound state of the atom makes $f^{(0)}_{RHS}(\omega, r)$ vanish, for the second order equation ($n = 2$) the driven term depends on $\varphi^{(1)}_l(\omega, r)$ which does not decay. This means that the source term is forcing the electron to follow the field in the whole space. Beyond a given value of the coordinate r, the first order solution $\varphi^{(1)}_l(\omega, r)$ reaches its asymptotic behavior. The action of the field gives an asymptotic behavior of the driven term which must be produced by the action of $[w_{sc} - H_0]$ on $\varphi^{(2)}_l(\omega, r)$. This leads to a similar analysis as for the first order: the spatial region to be solved is that where the driven term changes, i.e., before reaching its asymptotic behavior. This means that the basis functions to be used must be well defined in the inner region where the source term really changes. As illustrated in the next section, basis functions with an appropriately chosen asymptotic behavior are ideal to describe the solution.

3 Results

Let us consider the photoionization of the H atom initially in its ground state ($l_i = m_i = 0$); the exact wave function is $\overline{\Phi}^{(0)}(\mathbf{r}) = Z\sqrt{Z/\pi}e^{-Zr}$ and the ionization potential $E_I = 0.5$ a.u. In the case of a one photon absorption, the dipolar selection rule [25] imposes only one final angular momentum, $l = 1$, for the photoelectron. If the latter absorbs a second photon, the only possible values for the final angular momentum are either $l = 0$ or $l = 2$.

We solved the TISE (8) for the one-photon and two-photon ionization cases, and for photoelectron energies in the $(0.50, 8.00)$ a.u. range. We consider the interaction with an electric field whose characteristics are a linear polarization along the $\hat{z}$ direction, a laser frequency $\omega_{\mathcal{L}} = 3.37$ a.u. (photon energy $E_{\mathcal{L}} = 91.70$ eV) and an electric amplitude $\mathcal{E}_{\mathcal{L}} = 0.075$ a.u. (intensity $I_{\mathcal{L}} = 2 \times 10^{14}$ W/cm^2). The chosen parameters correspond to a ponderomotive energy $U_p = (\mathcal{E}_{\mathcal{L}}/2\omega_{\mathcal{L}})^2 = 1.24 \times 10^{-5}$ a.u. much smaller than $\omega_{\mathcal{L}}$, so that perturbation theory applies well. Furthermore, since the Keldysh parameter

$\gamma = \sqrt{E_I/2U_p} = 44.93$ is much larger than 1, the system is considered to be in the multiphoton regime.

We investigate first the case of a pulse and then of a monochrome laser.

3.1 Pulse

We consider a cosine-like electric field

$$\mathcal{E}(t) = \begin{cases} \mathcal{E}_{\mathcal{L}} \sin^2\left(\frac{\pi\, t}{\tau}\right) \cos\left(\omega_{\mathcal{L}}\, t\right) \hat{z}, & \text{if } 0 \le t \le \tau \\ 0, & \text{elsewhere} \end{cases} \tag{20}$$

with a sine-square envelope of time duration $\tau = 18.61$ a.u. ($\approx$450 as), which corresponds to a pulse of $n_c = 10$ optical cycles.

3.1.1 One-photon ionization

We use first the one photon absorption case to validate our methodology. Only $l = 1$ is possible, and we need to solve the driven equation (8) with $n = 1$. The driven term $f^{(0)}_{RHS}(\omega, r)$, which corresponds to the RHS of equation (6a), reads

$$f^{(0)}_{RHS}(\omega, r) = -\overline{\mathcal{F}}(\omega) \sqrt{\frac{4Z^5}{3}}\, r\, e^{-Zr}\, \delta_{l,1}\, \delta_{m,0}, \tag{21}$$

and is negligible beyond $r = 10$ a.u. To solve this radial TISE, we used a basis of 30 GSF obtained by setting in equation (9) $l = 1$, taking as generating potential a Yukawa potential $\mathcal{V}(r) = e^{-a\,r}/r$ with parameter $a = 0.01$, fixing the parameter E_s to be the photoelectron energy and imposing outgoing flux conditions (14) at $r = 30$ a.u.

At first order, from equation (17) and using equation (16), we have the one-photon DIP

$$\frac{dP_1(\omega)}{d\Omega} = \frac{4}{3}(2\pi)k_{sc}\left|C^{(1)}(\mathbf{k})\right|^2 = \frac{4}{3}(2\pi)k_{sc}\left|\sum_j a^{(1)}_{j,1}(\omega)\right|^2 \tag{22}$$

The ionization amplitude is related to the transition matrix elements by:

$$\begin{aligned} C^{(1)}(\mathbf{k}) &= i\,(2\pi)^{-1/2}\,\overline{\mathcal{F}}(\omega)\; T_1 \\ &= i\,(2\pi)^{-1/2}\,\overline{\mathcal{F}}(\omega)\left\langle \overline{\Phi}^{(1)} \left| (\hat{z}\cdot\nabla) \right| \overline{\Phi}^{(0)} \right\rangle, \end{aligned} \tag{23}$$

so that, from equation (18), the one-photon CS reads

$$\frac{d\sigma_1(\omega)}{d\Omega} = \frac{(2\,\pi)^3\,\alpha\, k_{sc}}{\omega} \frac{\left|\sum_j a^{(1)}_{j,1}(\omega)\right|^2}{\left|\mathcal{F}(\omega)\right|^2}. \tag{24}$$

The evaluation of these quantities is straightforward once the expansion coefficients $a^{(1)}_{j,1}(\omega)$ are obtained. The DIP results and the photoionization CS are presented in Figures 1 and 2 respectively, and show perfect agreement with analytical results. The width of the ATI dominant peak corresponds to the Fourier transform pulse width. The satellite peaks on both sides result from the fact that the density of probability is proportional to the square of the Fourier transform of the sine-square envelope (see discussion of Fig. 5). Gasaneo and Ancarani [32] gave the analytical expression of the solution $\varphi^{(1)}_l(\omega, r)$ with which one can deduce the ionization amplitude, and thus the DIP (Fig. 1) and the CS. In Figure 2 the CS comparison is made with the exact (more compact) analytical formula given by Harriman [33,34]. We mention that an excellent agreement is also found with results obtained by solving the TDSE [35,36] (results not shown in Figs. 1 and 2).

This first simple case demonstrates the capacity of the GSF method to accurately solve the driven equation.

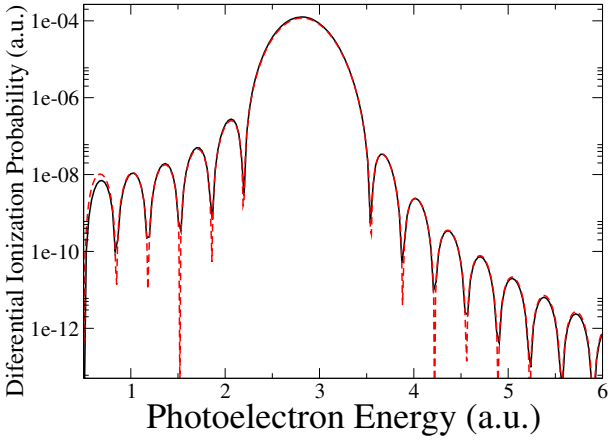

Fig. 1. One-photon ionization of H($1s$) atom by the pulse (20). Differential ionization probability as a function of the photoelectron energy: present GSF result (black solid line) and analytical [32] (red dashed line).

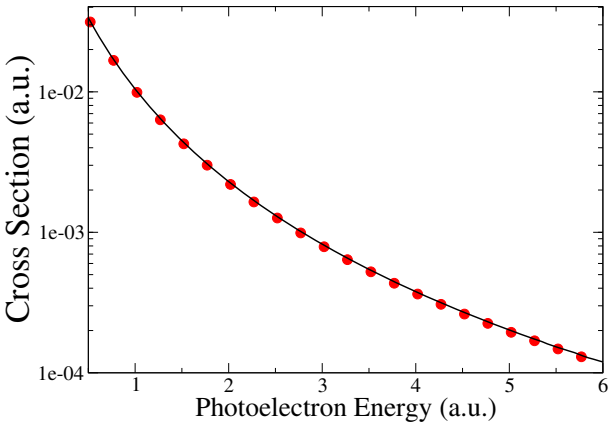

Fig. 2. One-photon ionization of H($1s$) atom by the pulse (20). Cross section as a function of the photoelectron energy: present GSF result (black solid line) and analytical [33] (red dots).

3.1.2 Two-photon ionization

For the two-photon ionization, after the system has absorbed the first photon, the photoelectron represented

by the outgoing radial function $\varphi_1^{(1)}(\omega, r)$ absorbs now a second photon. The radial equation describing this process is the driven equation (8) with $n = 2$ (corresponding to Eq. (6b)). The driven term $f_{RHS}^{(1)}(\omega, r)$ is slightly more complicated, but manageable; it reads

$$f_{RHS}^{(1)}(\omega, r) = \Delta_{l,m}^{-}\left[\mathcal{I}_{l-1,m}(\omega, r) - \frac{l(2l+3)}{2l+1}\mathcal{J}_{l-1,m}(\omega, r)\right] + \Delta_{l,m}^{+}\left[\mathcal{I}_{l+1,m}(\omega, r) - (1-l)\,\mathcal{J}_{l+1,m}(\omega, r)\right] - \sqrt{\frac{4Z^5}{3}}\overline{\mathcal{F}}(\omega)\, r\, e^{-Zr}\delta_{l,1}\delta_{m,0}, \quad (25)$$

where the functions

$$\mathcal{I}_{l,m}(\omega, r) = \frac{1}{\sqrt{2\pi}}\int_{-\infty}^{\infty} d\omega' \overline{\mathcal{F}}(\omega')\frac{d}{dr}\varphi_{l,m}^{(1)}(\omega - \omega', r)$$
$$\mathcal{J}_{l,m}(\omega, r) = \frac{1}{\sqrt{2\pi}}\int_{-\infty}^{\infty} d\omega' \overline{\mathcal{F}}(\omega')\frac{1}{r}\varphi_{l,m}^{(1)}(\omega - \omega', r),$$

involve the convolution of the electric field with the scattering wave function $\varphi_{l,m}^{(1)}$ and its first derivative. The quantities

$$\Delta_{l,m}^{-} = \sqrt{\frac{(2l+1) - (l^2 - m^2)}{(2l-1)}}$$
$$\Delta_{l,m}^{+} = \sqrt{\frac{(l+1)^2 - m^2}{(2l+1)(2l+3)}}$$

are constants for given quantum numbers l and m. We recall that by the dipolar selection rule the only possible values for the final angular momentum are $l = 0$ or $l = 2$.

Considering that the magnetic quantum number $m = 0$ is conserved, the driven term takes the form

$$f_{RHS}^{(1)}(\omega, r) = \int_{-\infty}^{\infty} d\omega'\, \overline{\mathcal{F}}(\omega')\left[p_l\frac{d}{dr}\varphi_1^{(1)}(\omega - \omega', r) - q_l\frac{1}{r}\varphi_1^{(1)}(\omega - \omega', r)\right] \quad (26)$$

where $p_0 = q_0 = 1/\sqrt{6\pi}$, $p_2 = \sqrt{10/27\pi}$ and $q_2 = (14/5)p_2$. The convolution of the non-decaying wave function $\varphi_l^{(1)}(\omega, r)$ with the pulse profile, leads to a two-photon driven term $f_{RHS}^{(1)}(\omega, r)$ that decays to zero asymptotically ($r \gtrsim 50$ a.u.), as illustrated in Figure 3. As a consequence, the solution to the $n = 2$ driven equation (8) will also have a Coulomb asymptotic behavior, and so will the scattering function up to second order

$$\overline{\Phi}_{\text{scatt}}(\omega, \mathbf{r}) = \overline{\Phi}^{(1)}(\omega, \mathbf{r}) + \lambda\overline{\Phi}^{(2)}(\omega, \mathbf{r}) \underset{r\to\infty}{\to} \left[\mathcal{A}_1^{(1)}(\omega)\mathrm{Y}_1^0(\theta)\lambda\Big(\mathcal{A}_0^{(2)}(\omega)\mathrm{Y}_0^0(\theta) + \mathcal{A}_2^{(2)}(\omega)\mathrm{Y}_2^0(\theta)\Big)\right]\frac{e^{i[k_{sc}r + (Z/k_{sc})\log(2k_{sc}r)]}}{r},$$

where λ is finally set to 1. We solved the driven equation for $l = 0$ and $l = 2$, respectively, using a basis composed of 128 GSF with outgoing flux conditions (14) imposed at $r = 75$ a.u., and a Yukawa generating potential with $a = 0.002$. The sum of the obtained coefficients $a_{j,0}^{(2)}(\omega)$ and $a_{j,2}^{(2)}(\omega)$ (see Eq. (16)), together with the corresponding angular weights, yields directly the two-photon ionization amplitude

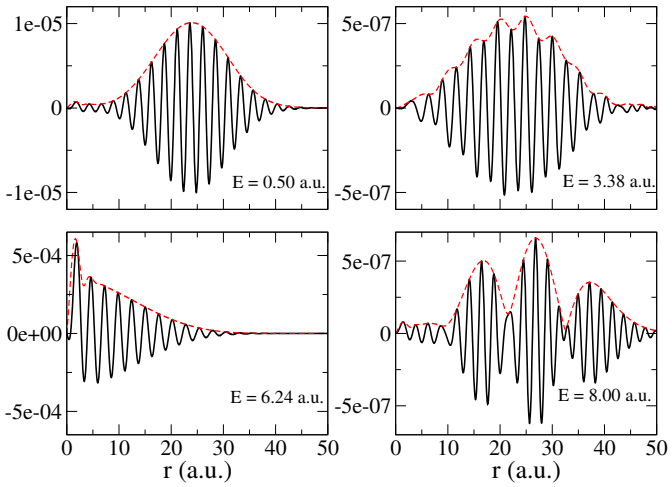

Fig. 3. Driven term $f_{RHS}^{(1)}(\omega, r)$ (Eq. (26)), for $l = 0$, and for 4 selected energies spanning the $[0.5, 8.0]$ a.u. range: real part (black line) and modulus (dashed red line).

$$C^{(2)}(\mathbf{k}) = \sum_j a_{0,j}^{(2)}(\omega)\,\mathrm{Y}_0^0(\theta) + \sum_j a_{2,j}^{(2)}(\omega)\,\mathrm{Y}_2^0(\theta). \quad (27)$$

Replacing the result into equation (17) and integrating angularly we obtain the two-photon DIP

$$P_2(\omega) = \frac{4}{3}(2\pi)k_{sc}\left(\left|\sum_j a_{0,j}^{(2)}(\omega)\right|^2 + \left|\sum_j a_{2,j}^{(2)}(\omega)\right|^2\right). \quad (28)$$

In Figure 4 we show our two-photon DIP and compare it with a TDSE calculation by Arbó [36]. A very good agreement between the two methods is observed. As expected, the spectrum exhibits the first two ATI peaks separated by the photon energy; the positions are given by $E_n = n\,\omega_{\mathcal{L}} - U_P - E_I \approx n\,\omega_{\mathcal{L}} - E_I$ (here, $E_1 = 2.87$ a.u. and $E_2 = 6.24$ a.u. for the first and second absorption, respectively). The first ATI peak, due to absorption of the first photon, is by far the dominant one. The differences in the second ATI peak region are due to the contributions of the channels not considered in the time-independent model. For further comparisons, both ATI peak energy regions are shaded. In Figure 5 we show the modulus of the Fourier transform of the pulse $\overline{\mathcal{F}}(\omega)$ (magenta solid line). Clearly, the pulse $\overline{\mathcal{F}}(\omega)$ displays a broad peak having exactly the same width as the first shaded region.

Following the proposal made in reference [28], we can perform a factorization of the two-photon ionization amplitude analogous to the first-order expression (Eq. (23)). For the second order, according to equation (19), the

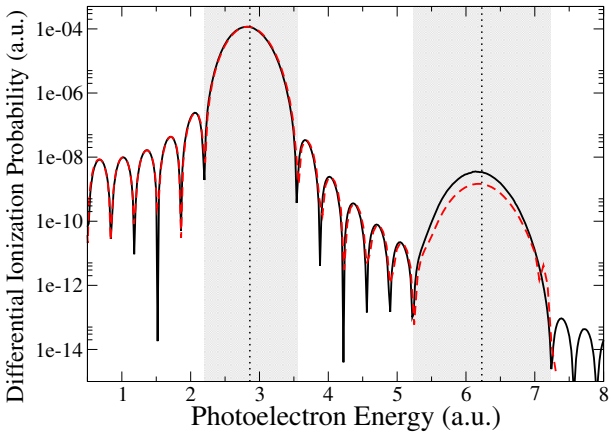

Fig. 4. Two-photon ionization of H($1s$) atom by the pulse (20). Differential ionization probability as a function of the photoelectron energy: present GSF results (black solid line) and time-dependent calculation by Arbó [36] (red dashed line). The vertical dotted lines indicate the first two ATI peaks.

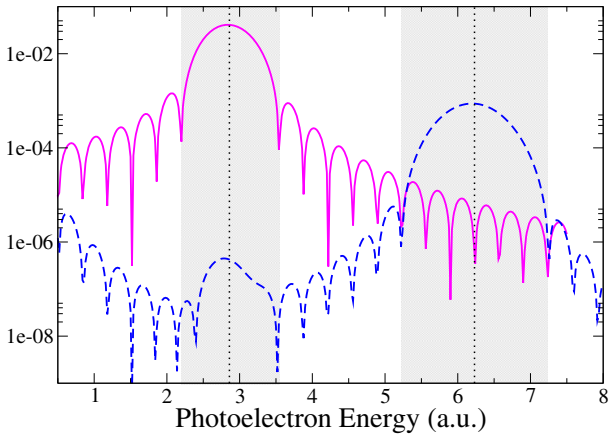

Fig. 5. Modulus of the Fourier transform of the pulse $\overline{\mathcal{F}}(\omega)$ (magenta solid line) and of the function $\overline{\Upsilon}(\omega)$ defined by equation (30) (blue dashed line) as a function of the photoelectron energy.

amplitude is expressed as:

$$C^{(2)}(\mathbf{k}) = -(2\pi)^{-3/2}\,\overline{\Upsilon}(\omega)\,T_2 = -(2\pi)^{-3/2}\,\overline{\Upsilon}(\omega)\left\langle \Phi^{(2)}\,|(\hat{z}\nabla) \times [\omega_i+\omega-H_0]^{-1}\,(\hat{z}\nabla)\Big|\,\Phi^{(0)}\right\rangle \tag{29}$$

where, in place of the pulse $\overline{\mathcal{F}}(\omega)$, the transition matrix is multiplied by the convolution function $\overline{\Upsilon}(\omega)$, defined by

$$\overline{\Upsilon}(\omega) = \int d\omega' \overline{\mathcal{F}}(\omega')\,\overline{\mathcal{F}}(\omega-\omega')\,. \tag{30}$$

In Figure 5 we also show the modulus of the convolution function $\overline{\Upsilon}(\omega)$ (blue dashed line), which presents a broad peak located at the same place and having exactly the same width as the shaded region conforming the second ATI peak. This correspondence suggests defining the two-photon ionization cross section within the bandwidth of the pulse as:

$$\frac{\sigma_2(\omega)}{I} = \frac{(2\pi)^6\,\alpha^2\,k_{sc}}{16\,\omega^3}\,\frac{\left(\left|\sum_j a^{(2)}_{0,j}(\omega)\right|^2 + \left|\sum_q a^{(2)}_{2,q}(\omega)\right|^2\right)}{\left|\overline{\Upsilon}(\omega)\right|^2} \tag{31}$$

which is valid only in the shaded region between 5.5 and 7.1 eV. We have calculated the cross sections resulting from both the TDSE and the GSF probabilities, displaying the results in Figure 6. Both cross sections show the same shape, and since the time-dependent calculation includes more ionization channels, the magnitudes are slightly different.

Finally, in Figure 7 we have plotted the cross section, differential in energy and in θ. It can be seen that the minimum of the angular distribution occurs at $\theta = 47.65°$, as it is well-known [37].

Our two-photon study and results confirm that, with our GSF methodology, we can successfully extract the ionization amplitude directly from the asymptotic limit of the scattering wave function, as already shown for the single-photon scenario.

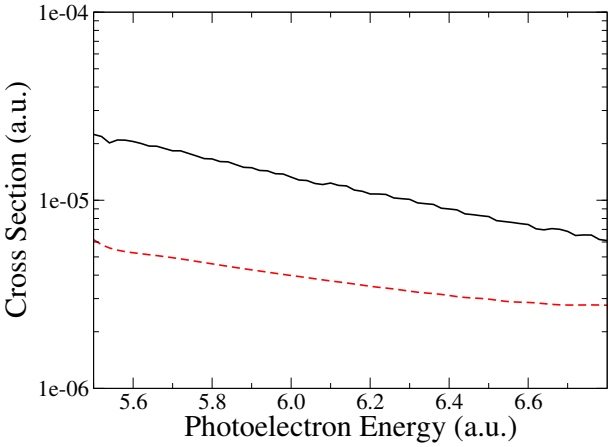

Fig. 6. Two-photon ionization of H($1s$) atom by the pulse (20). Cross section defined by (31) as a function of the photoelectron energy in the second ATI peak width: present GSF results (black solid line) and time-dependent calculation by Arbó [36] (red dashed line).

3.2 Laser

We now consider the two-photon ionization of the H atom by a monochrome laser of frequency $\omega_{\mathcal{L}}$. We choose linearly polarized light, with vector potential

$$\mathbf{A}(t) = A_{\mathcal{L}}\sin(\omega_{\mathcal{L}}\,t)\,\hat{z}, \tag{32}$$

i.e., with an envelope function equal to one. The Fourier transform $\overline{\mathcal{F}}(\omega)$ is now proportional to a delta function $\delta(\omega-\omega_{\mathcal{L}})$ so that the driven term (26) for the two-photon

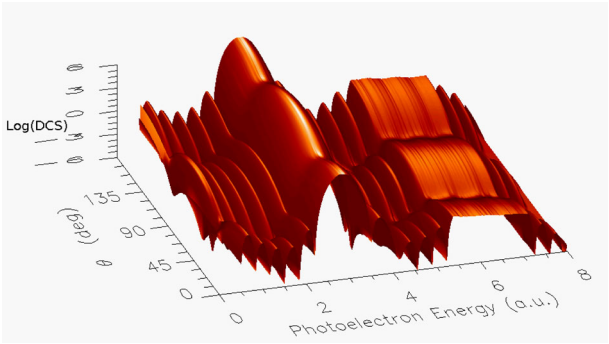

Fig. 7. Differential cross section, as a function of the photoelectron energy and angle θ, for the two-photon ionization of H($1s$) atom by the pulse (20).

ionization case, is simply

$$f^{(1)}_{RHS}(\omega,r) = A_{\mathcal{L}}\sqrt{\frac{\pi}{2}}\left(p_l\,\frac{d}{dr}\varphi^{(1)}_l(\omega-\omega_{\mathcal{L}},r) - q_l\,\frac{1}{r}\varphi^{(1)}_l(\omega-\omega_{\mathcal{L}},r)\right). \quad (33)$$

The one-photon scattering wave function $\varphi^{(1)}_l(\omega,r)$ has an outgoing Coulomb behavior at large distances; while the second term of $f^{(1)}_{RHS}(\omega,r)$ goes to zero asymptotically, the first one does not. This can be seen in Figure 8 where the real part of the driven term $f^{(1)}_{RHS}(\omega,r)$ for $l=2$ is plotted as a function of r. We thus have a situation which is very different from that observed in Figure 3 for the pulse case. The non-vanishing behavior enforces on the second order wave function $\varphi^{(2)}_l(\omega,r)$ a "beat" type asymptotic behavior. This is illustrated in Figure 9 where we show its real part for $l=2$: the asymptotic behavior is modulated by that of the source shown in Figure 8. The "beat" structure that appears beyond $r \gtrsim 15$ a.u. results from a linear combination of two Coulomb asymptotic behaviors

$$H^{(2)+}_{l,\infty}(r) = D_L\,H^{+}_{k_L,l}(r) + D_R\,H^{+}_{k_R,l}(r) \quad (34a)$$

$$\propto D_L\,e^{i[k_L r+(Z/k_L)\ln(2\,k_L r)]} + D_R\,e^{i[k_R r+(Z/k_R)\ln(2\,k_R r)]} \quad (34b)$$

one with $k_L = \sqrt{2\omega_{sc}}$ and the other with $k_R = \sqrt{2(\omega_{sc}-\omega_{\mathcal{L}})}$ corresponding to the energy of the LHS and RHS of equation (8), respectively. Similar forms (not shown) are obtained for the imaginary part and for the $l=0$ contribution.

Clearly, special care is needed when dealing with a non-vanishing driven term in the Schrödinger equation for the second photon absorption, and the "beat" asymptotic behavior of the scattering wave function needs a particular treatment [38]. Within our GSF approach we propose to tackle the problem through the following expansion

$$\varphi^{(2)}_l(\omega,r) = \sum_j c^{(2)}_{j,l}\;S_{j,l}(E_L,r) + \sum_j d^{(2)}_{j,l}\;S_{j,l}(E_R,r), \quad (35)$$

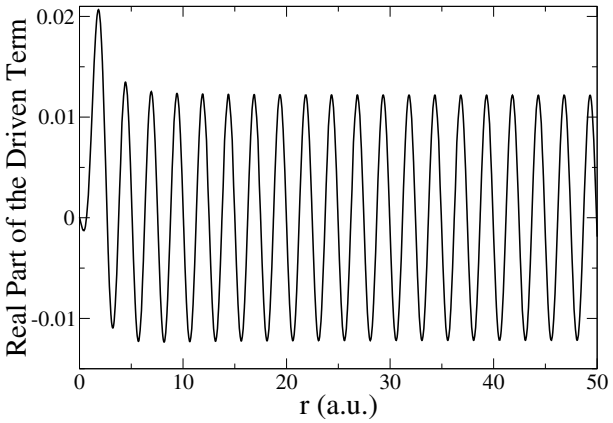

Fig. 8. Real part of the driven term $f^{(1)}_{RHS}(\omega,r)$, equation (33), for $l=2$, corresponding to case of the second photon absorption with a monochrome laser with a frequency $\omega = E_R = 3.14$ a.u.

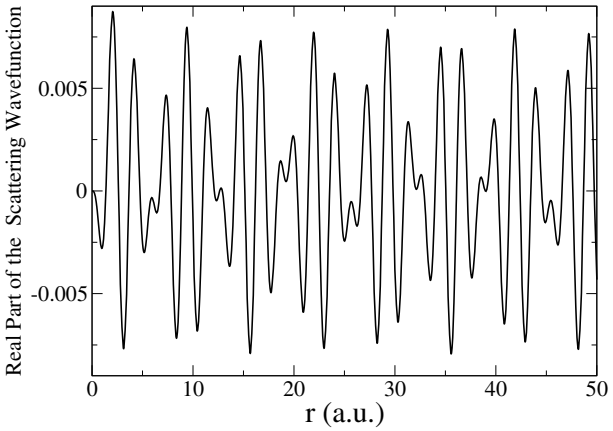

Fig. 9. Real part of the two-photon scattering wave function, $\varphi^{(2)}_2(\omega,r)$, for $l=2$.

i.e., in two sets of GSFs constructed with Coulomb asymptotic behaviors with appropriately chosen energy parameters $E_s = E_L = \omega_{sc}$ and $E_s = E_R = \omega_{sc}-\omega_{\mathcal{L}}$. For $r\to\infty$, we have

$$\varphi^{(2)}_l(\omega,r) \to \left(\sum_j c^{(2)}_{j,l}\right) e^{i[k_L r-(Z/k_L)\ln(2\,k_L r)]} + \left(\sum_j d^{(2)}_{j,l}\right) e^{i[k_R r-(Z/k_R)\ln(2\,k_R r)]} \quad (36)$$

providing the ionization amplitude $\mathcal{A}^{(2)}_l(\omega) = \sum_j c^{(2)}_{j,l}$ of the emitted photoelectron with scattering energy $\omega_i + 2\,\omega_{\mathcal{L}}$. As an example, in Figure 10, we show the two sets of GSFs and their linear combination. The Sturmian basis are constructed with a Yukawa generating potential with $a = 10^{-4}$, imposing a Coulomb asymptotic behavior at $r = 48$ a.u. with their respective energy, $E_s = E_L = \omega_{sc} = 6.01$ a.u. and $E_s = E_R = \omega_{sc}-\omega_{\mathcal{L}} = 3.14$ a.u. This linear combination results naturally in the "beat" asymptotic behavior (panel c) which matches,

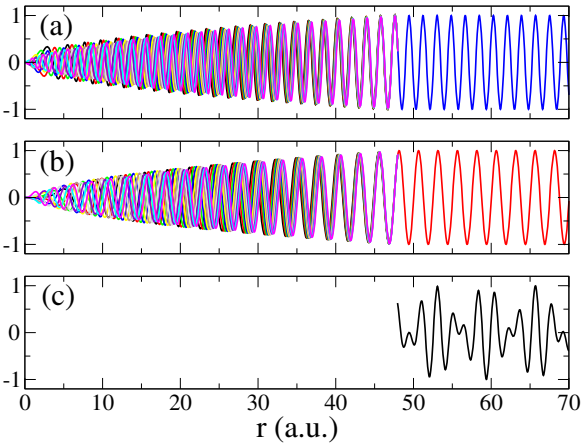

Fig. 10. For the case $l = 2$, real part of 10 basis functions: (a) Sturmian functions $S_{j,l}(E_L, r)$ with $E_s = E_L = \omega_{sc} = 6.01$ a.u. and an outgoing Coulomb asymptotic behavior imposed at $r = 48$ a.u.; (b) Sturmian functions $S_{j,l}(E_R, r)$ with $E_s = E_R = \omega_{sc} - \omega_{\mathcal{L}} = 3.14$ a.u. and an outgoing Coulomb asymptotic behavior imposed at $r = 48$ a.u.; (c) the linear combination of the previous two sets, shown for $r > 48$ a.u.

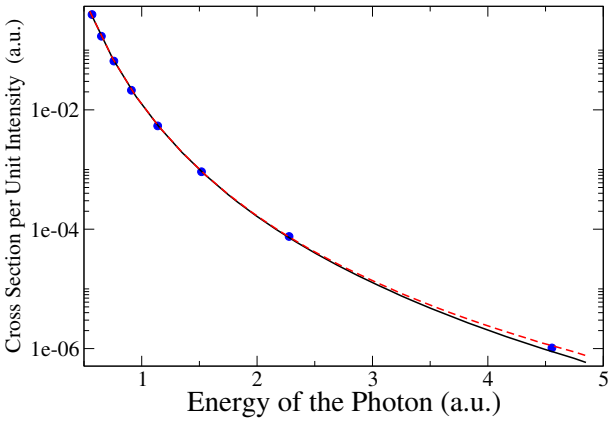

Fig. 11. Ionization rate for the two photon ATI of the H($1s$) atom interacting with a linearly polarized laser: blue dots, calculations by Karule and Moine [37]; our results obtained with the GSF method (red dashed line) and with the re-expansion in GSF of the scattering wave function calculated with a Green methodology (black solid line).

at large distances, the solution of the problem, presented in Figure 9.

In order to calculate the cross sections for the two-photon ionization of the H atom by a laser, we constructed the Sturmian basis with a Yukawa generating potential with $a = 10^{-4}$, imposing a Coulomb asymptotic behavior at $r = 75$ a.u. with their respective energy. We used a set of 70 GSFs with $E_s = E_L$ and the other with 10 GSFs with $E_s = E_R$. The CS is simply calculated as the sum of the coefficients belonging to the energy equal to the ejected electron. As observed in Figure 11, our results (red dashed line) are in good agreement with the ionization rate obtained by Karule and Moine [37] with the Coulomb Green Function method.

Another way to make use of the intrinsic properties of the GSF is as follows: the ionization amplitude can be derived from the scattering wave function $\varphi_l^{(2)}(\omega, r)$ obtained by any method up to a distance R. Here we calculated $\varphi_l^{(2)}(\omega, r)$ with an approach involving the Green operator for equation (8); we then re-expand it – in the range $r < R$ – into two set of GSFs constructed with Coulomb asymptotic behavior, with energies parameters $E_s = E_L$ and $E_s = E_R$, respectively (i.e., similarly to Eq. (35), but with different coefficients). The result shown in Figure 11 as a black solid line is again in good agreement with the other two data sets.

The difference between our two proposed schemes is at most of 1×10^{-7} a.u., indicating that both are valid. The advantage of the first scheme resides in the direct solution of the second order driven Schrödinger equation with two Sturmian basis sets with adequate intrinsic properties. The advantage of the second scheme, on the other hand, is that one may use the solution obtained with any other method and extract the scattering amplitude without requiring any projection, simply by using the GSFs properties.

4 Conclusion

We have developed a GSF methodology for multiphoton ATI resolution. We work within the framework of the time-independent Schrödinger equation and use a perturbative expansion of the scattering wave function; the resulting system of coupled driven equations allows one to analyze the process of absorption of one photon at a time above the ATI region. Our Generalized Sturmian scheme provides a very practical way to extract the transition amplitude directly from the asymptotic behavior of the scattering wave function. Using as a benchmark an hydrogen atom interacting either with a pulsed or a laser electric field, we have shown that the intrinsic properties of GSF one to evaluate the two-photon ionization amplitude simply as the sum of the coefficients of expansion without the need for any ad hoc approach. Comparisons with other very precise data (analytical or numerical) confirm the validity of our methodology.

One major difficulty that may arise when dealing with two-photon ionization is that the driven term of the corresponding non-homogeneous equation may not be spatially bound; special care must then be taken when solving it. For the one-photon ionization case, the target bound state always gives a bound driven term: the driven equation poses no particular numerical difficulty and can be solved with various methods. The resulting scattering wave function, with Coulomb outgoing wave condition, appears in the driven term of the next order driven equation which corresponds to absorption of a second photon. According to the nature of the electric field the target is subject to, the driven term of the two-photon non-homogeneous equation may not be bound and this requires special attention.

For the case of an interaction with a pulsed electric field, the two-photon ionization driven term remains bound, because of the convolution of the outgoing first order wave function with the pulse. The GSF strategy presented in previous papers [20,21] may therefore

be implemented as it is. Our one-photon differential ionization probability and ionization cross section are in perfect agreement with analytical results. Our two-photon differential ionization probability compares very well with that obtained with a time-dependent methodology by Arbó [36].

It is in the two-photon ionization case of the atom interacting with a laser that our methodology is of even greater value. The corresponding radial non-homogeneous equation involves a driven term of infinite spatial extension. We proved that this driven term forces a "beat" type asymptotic behavior in the scattering wave function associated with the absorption of the second photon. This beat behavior can be easily reproduced by appropriately chosen GSFs. We proposed to expand the scattering wave function on two sets of GSFs, built with different energy parameters: one set built with the energy of the emitted photoelectron and the other with the energy of the driven term. The two-photon ionization amplitude is extracted from the asymptotic limit of the wave function, directly as the sum of the expansion coefficients of the first GSF set, i.e., the one corresponding to the photoelectron energy. Furthermore, the intrinsic properties of the GSF allow one to extract the scattering amplitude directly from the wave function, regardless of the method by which it has been obtained and without calculating the transition matrix using some approximate final state. Very good agreement with published cross section is observed.

The methodology for multiphoton ATI resolution proposed here for the two-body case can be applied to both atoms and molecules (many-body case) interacting with an electric field. Its efficiency was demonstrated here for the hydrogen atom; the application to two-electron targets is currently under investigation. For the multiphoton double ionization of helium, for example, the first order solution of equation (6a) presents an hyperspherical wave front (see, e.g., [22]) and thus does not decrease at large distances. In the case of a monochrome laser, a non vanishing driven term is expected and treating the second order equation (6b) would require a special treatment, as the procedure presented in Section 3.2.

The authors thank the support by PGI (24/F049) of the Universidad Nacional del Sur, of ANPCyT (PICT08/0934) (Argentina), PIP 200901/552 and PIP 201301/607 of CONICET (Argentina). We also acknowledge the CNRS (PICS Project No. 06304) and CONICET (Project No. Dl 158114) for funding our French-Argentinian collaboration. We are grateful to Diego Arbó for providing unpublished data.

References

1. P. Sándor, V. Tagliamonti, A. Zhao, T. Rozgonyi, M. Ruckenbauer, P. Marquetand, T. Weinacht, Phys. Rev. Lett. **116**, 063002 (2016)
2. R.E. Goetz, A. Karamatskou, R. Santra, C.P. Koch, Phys. Rev. A **93**, 013413 (2016)
3. J. Miao, T. Ishikawa, I.K. Robinson, M.M. Murnane, Science **348**, 530 (2015)
4. H. Öström et al., Science **347**, 978 (2015)
5. L.J. Zipp, A. Natan, P.H. Bucksbaum, Optica **1**, 361 (2014)
6. M. Chini, K. Zhao, Z. Chang, Nat. Photon. **8**, 178 (2014)
7. K.T. Kim, D.M. Villeneuve, P.B. Corkum, Nat. Photon. **8**, 187 (2014)
8. F. Calegari, D. Ayuso, A. Trabattoni, L. Belshaw, S. De Camillis, S. Anumula, F. Frassetto, L. Poletto, A. Palacios, P. Decleva, J.B. Greenwood, F. Martín, M. Nisoli, Science **346**, 336 (2014)
9. C. Ott, A. Kaldun, P. Raith, K. Meyer, M. Laux, J. Evers, C.H. Keitel, C.H. Greene, T. Pfeifer, Science **340**,716 (2013)
10. K. Klünder, J.M. Dahlström, M. Gisselbrecht, T. Fordell, M. Swoboda, D. Guénot, P. Johnsson, J. Caillat, J. Mauritsson, A. Maquet, R. Taïeb, A. L'Huillier, Phys. Rev. Lett. **106**, 143002 (2011)
11. J. Mauritsson, T. Remetter, M. Swoboda, K. Klünder, A. LHuillier, K.J. Schafer, O. Ghafur, F. Kelkensberg, W. Siu, P. Johnsson, M.J.J. Vrakking, I. Znakovskaya, T. Uphues, S. Zherebtsov, M.F. Kling, F. Lepine, E. Benedetti, F. Ferrari, G. Sansone, M. Nisoli, Phys. Rev. Lett. **105**, 053001 (2010)
12. P. Emma, K. Bane, M. Cornacchia, Z. Huang, H. Schlarb, G. Stupakov, D. Walz, Phys. Rev. Lett. **92**, 074801 (2004)
13. C.M. Granados-Castro, L.U. Ancarani, G. Gasaneo, D.M. Mitnik, Adv. Quantum Chem. **73**, 3 (2016)
14. Th. Weber, H. Giessen, M. Weckenbrock, G. Urbasch, A. Staudte, L. Spielberger, O. Jagutzki, V. Mergel, M. Vollmer, R. Dröner, Nature **405**, 658 (2000)
15. E. Goulielmakis, Z. Loh, A. Wirth, R. Santra, N. Rohringer, V.S. Yakovlev, S. Zherebtsov, T. Pfeifer, A.M. Azzeer, M.F. Kling, S.R. Leone, F. Krausz, Nature **466**, 739 (2010)
16. M. Holler, F. Schapper, L. Gallmann, U. Keller, Phys. Rev. Lett. **106**, 123601 (2011)
17. C. Ott, A. Kaldun, L. Argenti, P. Raith, K. Meyer, M. Laux, Y. Zhang, A. Blattermann, S. Hagstotz, T. Ding, R. Heck, J. Madroñero, F. Martín, T. Pfeifer, Nature **516**, 374 (2014)
18. M.G. Pullen, W.C. Wallace, D.E. Laban, A.J. Palmer,G.F. Hanne, A.N. Grum-Grzhimailo, K. Bartschat, I. Ivanov, A. Kheifets, D. Wells, H.M. Quiney, X.M. Tong, I.V. Litvinyuk, R.T. Sang, D. Kielpinski, Phys. Rev. A **87**, 053411 (2013)
19. D.A. Horner, F. Morales, T.N. Rescigno, F. Martín, W. McCurdy, Phys. Rev. A **76**, 030701(R) (2007)
20. G. Gasaneo, L.U. Ancarani, D.M. Mitnik, J.M. Randazzo, A.L. Frapiccini, F.D. Colavecchia, Adv. Quantum Chem. **67**, 153 (2013)
21. D.M. Mitnik, F.D. Colavecchia, G. Gasaneo, J.M. Randazzo, Comp. Phys. Commun. **182**, 1145 (2011)
22. J.M. Randazzo, D.M. Mitnik, G. Gasaneo, L.U. Ancarani, F.D. Colavecchia, Eur. Phys. J. D **69**, 189 (2015)
23. L. Malegat, H. Bachau, A. Hamido, B. Piraux, J. Phys. B **43**, 245601 (2010)
24. L. Malegat, P. Selles, A. Kazansky, Phys. Rev. A**60**, 3667 (1999)
25. B.H. Bransden, C.J. Joachain, *Physics of Atoms and Molecules*, 2nd edn. (Pearson Education Limited, Malaysia, 2003)
26. M. Karplus, H.J. Kolker, J. Chem. Phys. **39**, 1493 (1963)

27. P.W. Langhoff, S.T. Epstein, M. Karplus, Rev. Mod. Phys. **3**, 602 (1972)
28. A. Palacios, C.W. McCurdy, T.N. Rescigno, Phys. Rev. A **76**, 043420 (2007)
29. A. Palacios, C.W. McCurdy, T.N. Rescigno, Phys. Rev. A **77**, 032716 (2008)
30. C.M. Granados-Castro, J.L. Sanz-Vicario, J. Phys. B **46**, 055601 (2013)
31. F.H.M. Faisal, *Theory of Multiphoton Processes*, 2nd edn. (Springer Science & Business Media, New York, 1987)
32. G. Gasaneo, L.U. Ancarani, in Press
33. J.M. Harriman, Phys. Rev. **101**, 594 (1956)
34. T.N. Rescigno, V. McKoy, Phys. Rev. A **12**, 522 (1975)
35. J.L. Sanz-Vicario, A. Palacios, J.C. Cardona, H. Bachau, F. Martín, J. Electron Spectrosc. Relat. Phenom. **161**, 182 (2007)
36. D.G. Arbó, private communication
37. E. Karule, B. Moine, J. Phys. B **36**, 1963 (2003)
38. M.J. Ambrosio, L.U. Ancarani, A.I. Gómez, G. Gasaneo, D.M. Mitnik, submitted to J. Math. Phys.